Environmental Science Advances

ROYAL SOCIETY OF CHEMISTRY

PAPER

View Article Online
View Journal

Cite this: DOI: 10.1039/d5va00186b

Mechanical recycling of multiphase contaminated plastic waste *via* physical compatibilization: a study on rheological, morphological and mechanical properties

Hu Qiao, Geraldine Cabrera, Abderrahim Maazouz and Khalid Lamnawar *

During the recycling of polyethylene (PE)-based agricultural film waste, the presence of small amounts of polypropylene (PP)-containing films can significantly deteriorate the mechanical properties of the recycled material. This is primarily due to the immiscibility between PE and PP in such complex multiphase systems. Physical compatibilization is widely regarded as the most efficient and practical method for improving mechanical performance and interfacial adhesion in such mechanically recycled multiphase waste systems. In this study, propylene–ethylene elastomer (EPR) and ethylene–octene copolymer (EOC) were selected as physical compatibilizers for both binary model PE/PP blends and quaternary model recycled PEs/PPs blends. The blends consisted of virgin LLDPE, LDPE, and their mixtures as the major phase, combined with 10 wt% PP as the minor phase and 7% compatibilizer. The specific research strategy was to enhance mechanical performance in the presence of physical compatibilizers by inducing and/or modifying the morphological structures within the blends, supported by rheological analysis. The compatibilization effects were initially investigated through rheological and morphological analyses. A decrease in complex viscosity and storage modulus, particularly at lower frequencies, was found in small-amplitude oscillatory shear (SAOS) rheology, indicating improved interfacial compatibility between PE and PP. These findings were further supported by scanning electron microscopy (SEM) and transmission electron microscopy (TEM), which revealed finer morphologies and significantly reduced dispersed domain sizes in both compatibilized systems. As a result of enhanced interfacial adhesion and the elastic features of the compatibilizers, notable improvements in impact resistance, tear resistance, and elongation at break were achieved. In summary, compared to EPR, EOC demonstrated superior compatibilization performance in the recycled blends, likely due to its ethylene/octene segmental structure, which exhibits greater chemical affinity with polyethylene. The ultimate target is to guide the mechanical recycling of contaminated plastic waste through establishing rheology-morphology-property relationships in complex multiphase systems. This study offers valuable insights into effective compatibilization strategies for complex multiphase polymer recycling systems.

Received 24th June 2025
Accepted 23rd September 2025

DOI: 10.1039/d5va00186b

rsc.li/esadvances

Environmental significance

This study supports sustainable plastic waste management by improving the mechanical recycling of polyethylene (PE)-based agricultural film waste contaminated with polypropylene (PP). Through physical compatibilization using ethylene–octene copolymer (EOC) and propylene–ethylene elastomer (EPR), the research enhances interfacial adhesion and mechanical properties in multiphase recycled blends. The improved recycling process reduces plastic waste, promotes material reuse, and minimizes environmental pollution. EOC showed superior performance, offering a practical approach to managing mixed-polymer waste streams. These findings contribute to advancing circular economy practices and reducing the ecological footprint of agricultural plastics.

1 Introduction

In the recycling process of solid plastic waste (SPW), post-industrial (PI) waste is generally considered to be of higher-quality level, as it is clean, has a well-known composition, and can be easily re-used within the same production facilities.[1,2] By contrast, as expected, post-consumer (PC) plastic waste is more challenging to separate and recycle due to its heterogeneous unknown composition and potential contamination.[3] In addition to non-packaging PC waste, agricultural plastic waste (APW) has significantly contributed to the accumulation of plastic waste in rural areas over the past few decades. This trend

Universite Claude Bernard Lyon 1, INSA Lyon, Université Jean Monnet, CNRS UMR 5223, Ingénierie des Matériaux Polymères F-69621, Villeurbanne Cédex, France. E-mail: khalid.lamnawar@insa-lyon.fr

is largely driven by the growing and widespread use of plastics in agriculture, with an estimated 2–3 million tons of plastics consumed annually for agricultural purposes. Nearly half of this total agricultural plastic films are used in protective cultivation, such as mulching, greenhouses, small tunnels, temporary coverings for fruit trees, *etc.*[4] These applications help to increase yields, earlier harvests, reduced reliance on herbicides and pesticides, better protection of food products, and more efficient water conservation. The remaining portion is primarily applied in livestock farming, including silage, bale wrapping, and protection films.[5] However, in recent years, the majority of APW has been either directly landfilled or burnt uncontrollably by farmers. These disposal practices are harmful to the environment, pose risks to human health, and compromise the safety of farming products.[5]

Overall, mechanical recycling remains the most widely used technique for processing solid plastic waste (SPW), including both PI and PC waste. Mechanically recycled plastics can closely approximate the original or virgin materials, making them suitable as secondary raw materials for the production of high value-added products.[6,7] In agriculture plastic films, two polyethylene-based polymers, linear low-density polyethylene (LLDPE) and lower density polyethylene (LDPE), are the most commonly used.[8] However, the waste stream from PE-based agricultural films is often contaminated by agrochemical containers made of various types of polypropylene (PP).[9] Consequently, mixed and contaminated plastic waste containing LLDPE, LDPE, and small amounts of PP is frequently found in recycling streams, and these materials are typically processed together during mechanical recycling. So far, none of these automatic sorting procedures are sufficiently effective to completely separate polyethylene from polypropylene, particularly when the PP content ranges from 5 wt% to 10 wt%. In addition to the unknown compositions, the presence of PP phases in multiphase systems leads to the incompatibility between polymer phases, thereby reducing the mechanical properties of the recycled material. This does not allow the recovery of high-quality film materials and significantly diminishes the value of the recycled products.

Numerous studies have investigated the various properties of virgin and recycled model PE/PP blend with varying compositions. As expected, due to inherent incompatibility and immiscibility between PP and PE, the incorporation of 5–30 wt% PP into PE matrix significantly deteriorates the mechanical performance of the resulting blends. This is evidenced by a remarkable reduction in the elongation at break and impact strength of the PE matrix. Although an increase in Young's modulus and tensile strength at yield can be observed, the resulting recycled blends become more rigid and brittle compared to neat PE or compatible PE-based blends, and thus fail to replicate the flexibility of virgin film materials.[10] The incompatibility between PE and PP has been well demonstrated, primarily through microscopic and calorimetric analyses.[11,12] Two-phase separation is consistently observed across the entire composition range of PE/PP mixtures. Specifically, when PE is the major component, the PP phase typically displays a droplet-like morphology dispersed within the continuous PE matrix. The poor mechanical properties of these blends can be primarily attributed to the weak interfacial affinity and adhesion between the two phases, which are closely associated with their phase morphology.

In case of partially miscible or immiscible blends, it is well known that factors such as composition, individual rheological properties, processing conditions, and thermodynamic interactions in the molten state significantly influence the morphology and compatibility of the blends.[13] Consequently, considerable efforts have been made to enhance the compatibility between polyethylene (PE) and polypropylene (PP). According to the literature, the incorporation of compatibilizers is the most efficient and practical strategy for improving compatibility and morphological dispersion. This is achieved by reducing interfacial tension and strengthening adhesion between polymer phases, thereby enhancing the mechanical properties of the recycled blends. Kazemi *et al.* (2015) summarized the most common used graft or block copolymers as compatibilizers for PE/PP blends. These include styrenic block copolymers (SCB), ethylene–propylene elastomers (EPR), ethylene–propylene-diene copolymer (EPDM), ethylene–vinyl acetate (EVA) and ethylene–octene copolymers (EOC), *etc.*[14] These compatibilizers contain segments structurally similar to the blend components (PE and PP), achieving compatibilization through the physical affinity of the blocks with each polymer phase, which results in an improvement in interfacial adhesion. In particular, two types of representative compatibilizers, ethylene–propylene elastomers (EPR) and ethylene–octene copolymers (EOC), are expected to be highly effective in compatibilizing PE/PP blends and enhancing the mechanical performance of the final products. Although the model binary PE/PP system has been extensively studied, to the best of our knowledge, there are few reports that specifically address complex multiphase PEs/PPs systems. Therefore, multiphase blends and their compatibilized systems, with a specific composition designed to simulate mixed, contaminated plastic waste, should be systematically investigated.

In this study, mixed contaminated agricultural plastic waste, containing LLDPE and LDPE blend as the major components, homo-PP (HPP) and copo-PP (CPP) as the dispersed phase, were selected as polymer matrix. Specifically, this quaternary model recycled blend incorporating a total of 90 wt% LLDPE/LDPE and 10 wt% CPP/HPP was prepared *via* mechanical recycling, followed by films blowing. For comparison, model binary PE/PP blends were also investigated to provide fundamental insights. Subsequently, two representative compatibilizers, ethylene–propylene elastomers (EPR) and ethylene–octene copolymers (EOC), were mixed into the blends to evaluate their physical compatibilization effects. Our research aims to develop a deeper understanding of the structure–property relationships in complex multiphase systems. The effect of physical compatibilization on enhancing mechanical properties was systematically investigated by inducing and/or generating specific morphological structures within the blends, further supported by rheological analyses. Accordingly, the compatibilization behavior in multiphase PE/PP systems was evaluated using small-amplitude oscillatory shear (SAOS) rheological

measurements. The resulting rheological properties and predicted morphologies were then corroborated through morphological characterization using scanning electron microscopy (SEM) and transmission electron microscopy (TEM). Subsequently, the mechanical performance of the blends, including the impact, tear and tensile properties, was comprehensively measured. In summary, the introduction of two types of compatibilizers significantly improved the compatibility of the quaternary PE/PP blends. This improvement was evidenced by reduced interfacial tension and elastic modulus, a notable decrease in droplet size of dispersed phase, and enhanced mechanical properties. Among the two, EOC demonstrated the most effective compatibilization effect, which can be attributed to its molecular structure of ethylene–octene segment that is chemically similar to polyethylene. This study offers valuable insights for enhancing the mechanical performance of complex plastic waste streams through mechanical recycling, particularly in application-specific industrial scenario.

2 Experimental section

2.1 Materials and formulations

As previously discussed, the recycled materials obtained through the mechanical recycling of multilayer films consist of LLDPE and LDPE, along with a PP content ranging from 5 wt% to 10 wt%. Accordingly, virgin LLDPE, LDPE and two types of PP were used to prepare model recycled blends, as listed in Table 1. In addition, two types of compatibilizers, propylene–ethylene elastomer (EPR) and ethylene–octene copolymer (EOC), were selected to enhance the interfacial adhesion between PEs and PPs phase, due to their similar segments as the blend components.

To best simulate practical formulations derived from the agricultural waste streams entering the mechanical recycling process, a model recycled blend (MR1) was designed using LLDPE and LDPE in equal proportions, with a total of 10 wt% PP (5 wt% HPP and 5 wt% CPP). Based on this uncompatibilized blend (MR1), two compatibilized model recycled blends were also prepared: MR2, incorporating 7 wt% propylene–ethylene rubber (PER), and MR3, incorporating 7 wt% ethylene–octene copolymer (EOC), as summarized in Table 2. Prior to the model recycling study, biphasic PE/PP model blends (LDPE/HPP and LLDPE/CPP) with or without compatibilizers were prepared to independently investigate the compatibilization effects between individual PE/PP blends, as shown in Table 3.

Table 2 Formulations showing compositions of model recycled blends with or without compatibilizers

Blend	LLDPE/LDPE (wt%/wt%)	HPP/CPP (wt%/wt%)	EPR (wt%)	EOC (wt%)
MR1	45/45	5/5	—	—
MR2	41.5/41.5	5/5	7	—
MR3	41.5/41.5	5/5	—	7

2.2 Sample preparation: compounding extrusion of blends and blown extrusion of monolayer films

All blends were prepared using a two-step extrusion process, compounding extrusion of blends and blown extrusion of monolayer films. Firstly, blend compounding was performed using a co-rotating twin-screw extruder (L/D = 77). The specific twin-screw profile is shown in Fig. 1, with detailed process parameters provided in Table 4. All formulations, as shown in Tables 2 and 3, were processed under identical processing parameters, with a temperature profile ranging from 180 °C to 200 °C, a constant feed rate, and a screws speed of 70–75 rpm. The extrudate was finally quenched in a cold-water bath, followed by drying and pelletizing using a cutting machine.

Monolayers films of the blends were produced *via* blown film extrusion using a 50 mm annular blow die coupled to a co-rotating twin-screw extruder with a clam-shell barrel design and a length/diameter ratio of 25 : 1 (Thermo Electron Polylab System Rhecord RC400P, Courtaboeuf, France). The extrusion temperature profile was gradually increased from 190 °C at the feeding zone to 220 °C at the pumping zone. The molten polymer in the form of a tube exited from the die at 220 °C, which was then drawn upward by a take-up device. During starts-up, air was introduced at the bottom of the die to inflate the tube, forming a bubble. The bubble was subsequently flattened by nip rolls and collected by a winder. An air ring was used to rapidly cool and solidify the hot bubble above the die exit. The film dimensions were determined by the Blow-Up Ratio (BUR) and Take-Up Ratio (TUR). BUR is defined as the ratio between the final bubble diameter (D_f) to the die diameter (D_0), controlled by varying the air pressures. TUR is the ratio of the speed of the take-up device (V_f) and the extruded material velocity (V_0) at the die exit. All monolayer films, corresponding to the formulation in Tables 2 and 3, were obtained under identical extrusion parameters, with a drawing speed of 3.7 m min^{-1} and fixed BUR

Table 1 Characteristics of the Polyethylene, Polypropylene and their compatibilizers used in this study

Polymer	LLDPE	LDPE	HPP	CPP	EPR	EOC
Manufacturer	Chevron Phillips	Eni Versalis	Lyon dellBasell	Lyon dellBasell	Exxon Mobil	Dow chemical
Monomer type	Copolymer ethylene/ L-hexene	Ethylene	Homopolymer PP	Copolymer propylene/ ethylene	Propylene/ ethylene elastomer	Ethylene/ octene copolymer
Density (g cm^{-3})	0.918	0.924	0.900	0.900	0.862	0.875
MFI (g/10 min)	1.0[a]	0.25[a]	3.4[b]	0.85[b]	1.3[a]	1.0[a]

[a] 190 °C/2.16 kg. [b] 230 °C/2.16 kg.

Table 3 Formulations showing compositions of model PE/PP blends and their compatibilized blends

Blend	LLDPE (wt%)	LDPE (wt%)	HPP (wt%)	CPP (wt%)	EPR (wt%)	EOC (wt%)
M1	90	—	—	10	—	—
M2	83	—	—	10	7	—
M3	83	—	—	10	—	7
M4	—	90	10	—	—	—
M5	—	83	10	—	7	—
M6	—	83	10	—	—	7

and TUR settings, resulting in films with a thickness of approximately 30 ± 5 μm.

3 Characterizations

3.1 Small amplitude oscillatory shear (SAOS) rheology

The liner viscoelastic properties of all blends were evaluated using dynamic frequency sweeps measurements within the linear viscoelastic region. The experiments were performed on a stress-controlled rheometer (Discovery Hybrid Rheometer, DHR-2, TA Instruments) equipped with a plate–plate configuration (Φ = 25 mm) at 200 °C under a nitrogen atmosphere. Disk-shaped specimens were positioned between the plates with a gap inferior to 1.5 mm. Before the measurement, samples were held at the testing temperature for approximately 3 min to ensure complete melt relaxation. Frequency sweeps were then performed from the high angular frequency (ω) of 628 down to low 0.314 rad s^{-1}, at a fixed strain amplitude of 2% in the linear viscoelastic regime, with five data points collected per decade.

3.2 Morphological observation

The morphologies of both model-recycled and virgin blends were evaluated using Scanning Electron Microscopy (SEM) and Transmission Electron Microscopy (TEM). For the SEM analysis, cross-fractured surfaces were prepared by immersing the samples in liquid nitrogen for a brittle fracture treatment. Additionally, smooth surfaces of the sample were obtained using a cryoultramicrotome (LEICA UC7) under liquid nitrogen atmosphere. These surfaces were subsequently polished treatment and chemically stained with ruthenium tetroxide (Ru04) vapor for 2 hours to enhance the phase contrast. SEM observations of both fractured and surfaced samples were carried out using a FEI QUANTA 250 FEG microscope in two different operation models. In high-vacuum mode, samples were coated with a thin layer of carbon to prevent charging. In low-vacuum mode, samples were directly placed in standard SEM stubs using a conductive silver glue and performed at an operating voltage of 2 kV with an environmental secondary electron detector, which effectively minimized the electrical charging effects.

TEM analysis was performed using a Philips CM120 microscope with an operating voltage at 80 kV. The surface of samples was cut into an approximately thickness of 80 nm by the same operation as mentioned before. High-resolution TEM images were captured with a Gatan Orius camera.

3.3 Mechanical properties

Tear resistance and dart impact strength, the critical end-use tests for blown films, were performed to evaluate the effect of the compatibilizers on the mechanical properties of the recycled blends. In this study, the Elmendorf pendulum method (ISO 6383-2) was applied using an Elmendorf machine to determine the dynamic resistance of samples designed to be subjected to strong shearing loads. The blown film samples cut in both the machine direction (MD) and the transverse direction (TD) were fixed between the clamps, and then the pendulum at appropriate weight (400 g to 800 g) was applied and released to completely tear the specimen. The difference of the angle from the vertical center of the pendulum gravity between the downswing and the upswing is recorded as the energy absorbed in tearing sample. The angular value is measured and converted to the mean tearing force by the microprocessor incorporated in the machine (Testing Machines Inc 2020). An average tear force in Newton per five times was finally obtained for each sample.

Falling dart impact as a common method for evaluating the impact strength or toughness of a plastic film was performed using the Free-falling Dart Method (ISO 7765-1), specifically the "staircase" method of assessment to determine the energy required for failure of 50% of the specimens. The failure of the films was caused by a puncture due to the impact.

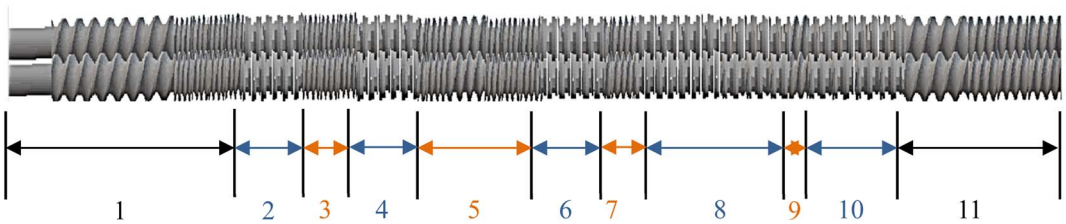

Fig. 1 Twin-screw profile used in the study.

Table 4 Description of the twin-screw profile and temperature

Zone (N°)	Description	Function	T (°C)
1	34.8 cm: Bi-lobed conveying elements	Feed/Compression	180
2	11.2 cm: 11 kneading blocks (30°) 5 kneading blocks (90°)	Mixing	200
3	7.2 cm: Bi-lobed conveying elements	Compression	200
4	5.9 cm: 5 kneading blocks (45°) 4 kneading blocks (60°)	Mixing	200
5	29.5 cm: Bi-lobed conveying elements	Compression + Venting	200
6	5.9 cm: 5 kneading blocks (45°) 4 kneading blocks (60°)	Mixing	200
7	4.0 cm: Bi-lobed conveying elements	Compression	200
8	6.6 cm: 5 kneading blocks (45°) 5 kneading blocks (60°)	Mixing	200
9	2.0 cm: Bi-lobed conveying elements	Compression + Venting	200
10	3.3 cm: 5 kneading blocks (45°)	Mixing	200
11	20.6 cm: Bi-lobed conveying elements	Transport	200

The tensile test of specimens in a rectangular shape in dimensions of 4 (±0.5) mm in width, and 50 (±0.1) mm of length (ISO 527-1) was performed with an electromechanical testing machine INSTRON. The end side of the specimen was held at a fixed position, while the other side was displaced at a constant rate of 50 mm min^{-1}, using a load cell of 100 N. The elongation and tensile strength at break were determined from the stress–strain plot.

4 Results and discussion

4.1 Effect of the compatibilizers on rheological properties

The linear viscoelastic properties of the blends were measured using small amplitude oscillatory shear (SAOS) rheology within the linear regions to evaluate the compatibility between multi-phases with or without compatibilizers. Fig. 2 presents the complex viscosity modulus (η^*) and storage modules (G') as a function of angular frequency at 200 °C for the neat polymers and LLDPE/CPP (90/10) blends with and without compatibilizers. As shown in Fig. 2(a) and (b), CPP exhibits higher viscosities at low angular frequencies and more pronounced shear-thinning behavior at the whole range of frequencies. This is attributed to its molecular structure containing a certain contents of ethylene units. In contrast, LLDPE displays a Newtonian plateau at low frequencies followed by pronounced shear-thinning behavior at higher frequencies. Notably, that compatibilizer EPR exhibits lower complex viscosity values than both polymer matrices at whole range of angular frequencies. This is primarily due to its elastomeric nature and relatively low molar mass.[14]

The addition of 10% CPP to LLDPE results in the pronounced upturn shift behavior in the complex viscosity at low frequencies. This is attributed to the additional tension at the interface caused by their immiscibility between the two polymers, which is further supported by the corresponding increase in storage modulus (G') at the same frequency zones. Consequently, the rheological behavior of LLDPE/CPP blend across the entire frequency spectrum is overall dominated by CPP phase. After the introduction of compatibilizer EPR, a significant decrease in both complex viscosity and storage modulus at lower frequencies is clearly observed. Moreover, the presence of EPR leads to a continuous decrease in viscosity of the LLDPE/CPP blends at the entire frequency range and the pronounced shear-thinning behavior at higher frequencies. These results indicate that EPR significantly improves the compatibility between LLDPE and CPP by reducing additional interfacial tension and minimizing unfavorable interactions from CPP phase. The propylene–ethylene segments of EPR display better affinity and adhesion with CPP phases.

In contrast, as shown in Fig. 2(c) and (d), the addition of another compatibilizer, EOC, negligibly influences the η^* and G′ of the blends at lower frequencies. However, at frequencies above 60 rad s^{-1}, a slight increase in η^* is observed, despite EOC itself exhibiting lower complex viscosities than both LLDPE and CPP at the entire frequency range. Unlike EPR, the presence of EOC appears to the negligible influence on the rheological properties of the blend, which may be attributed to the similar molecular structures of EOC and LLDPE, both of which are ethylene–octene copolymers and exhibit relatively low elasticity. Given that the LLDPE/CPP blend is predominantly influenced by the CPP phase, it is possible that EOC containing more ethylene structure slightly enhances the interactions between LLDPE and CPP. In contrast, EPR, incorporating more propylene-ethylene segments, exhibits greater compatibility with CPP phase, thereby promoting the better phase dispersion and reducing interfacial tension. These preliminary conclusions require to be further analyzed by combining complementary morphological observations.

Fig. 3 further displays the complex viscosity (η^*) and storage modules (G') depending on angular frequency at 200 °C for the LDPE/HPP blend pair with a huge difference in viscosity. As shown in Fig. 3(a) and (b), due to its long-chain branched molecular structure, LDPE presents higher viscosities at lower frequencies and a more pronounced shear-shining behavior at whole range of the frequency compared to less-branched HPP. With the addition of 10 wt% of less viscous HPP, the blend displays intermediate η^* and G' values between neat LDPE and HPP, accompanied by a notable decrease in complex viscosity

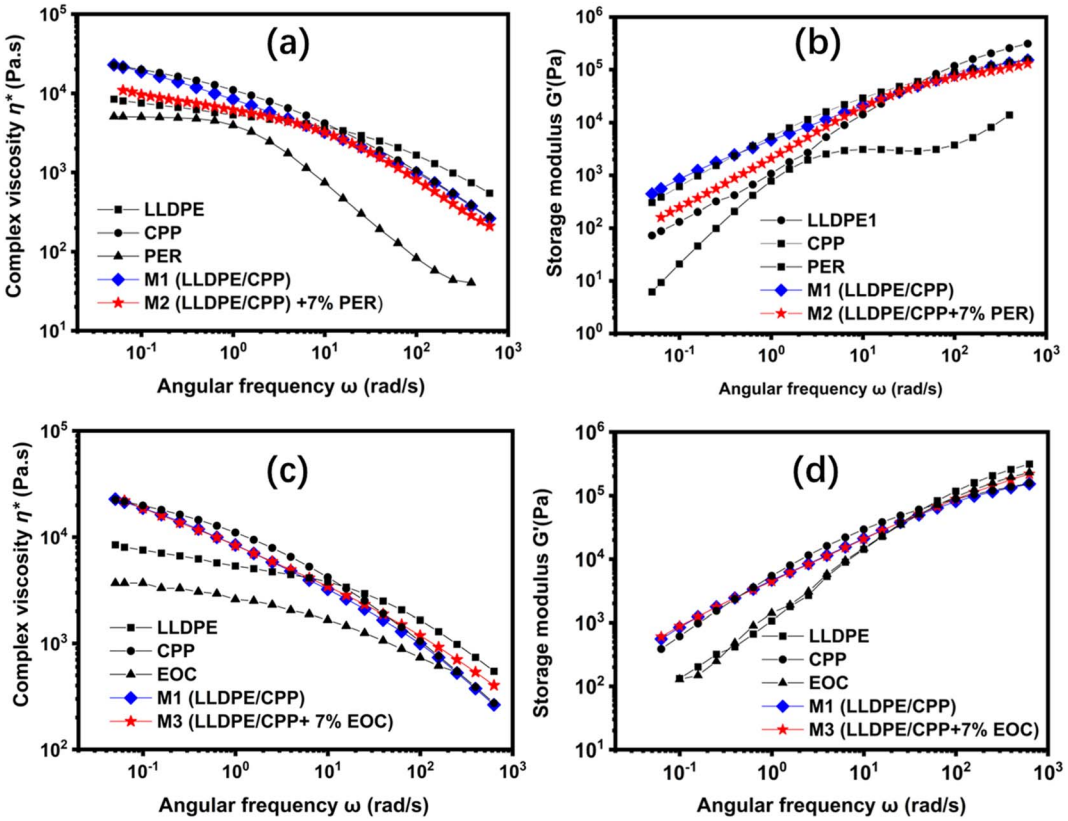

Fig. 2 Plots of complex viscosity (η^*) and storage modules (G') as functions of angular frequency at 200 °C for neat polymers, the LLDPE/CPP blend, and their compatibilized blends with EPR (a and b) and EOC (c and d).

relative to pure LDPE. This reduction is primarily attributed to the huge difference in viscosity between the two polymers. Upon incorporation of PER, the resulting blend shows minimal changes in both η^* and G' across all frequencies, indicating that PER has little effect on enhancing the interfacial interactions, likely due to its higher propylene content in its structure. In contrast, the EOC-compatibilized blend exhibits a less pronounced shear-thinning behavior in complex viscosity compared to uncompatibilized LDPE/HPP blend, present in Fig. 3(c) and (d). This is evidenced by a decrease in both η^* and G' at low frequencies and an increase at higher frequencies. These observations imply that EOC, due to its molecular structure of ethylene/octene copolymer, presents a strong affinity between LDPE and HPP through between interfacial interaction. Nevertheless, all blends with or without compatibilizer still present rheological properties intermediate between those of neat HPP and LDPE.

Finally, multiphases recycled blends incorporating LLDPE, LDPE, CPP and HPP at different compositions simulating the agricultural plastic films waste are investigated using small-amplitude oscillatory shear (SAOS) rheology and Han' plot. Specifically, the three model recycled blends (Table 2) consist of equal amounts of LLDPE and LDPE (50/50), with 10 wt% PP (5 wt% HPP and 5 wt% CPP) with or without 7 wt% compatibilizer. Although LLDPE/LDPE and HPP/CPP binary blend pairs present miscibility or partial miscibility, the quaternary blends are expected to be immiscible or partially miscible among components. As shown in Fig. 4, the MR1 blend, containing quaternary components, displays intermediate complex viscosity (η^*) and storage modules (G') values compared to the LLDPE/LDPE and CPP/HPP blends. This indicates that the rheological behavior of these multi-components blend systems is more simple composition-dependent due to complex interactions between phases. The compatibilized blend MR2 shows a slight decrease in both η^* and G' at higher frequencies but demonstrates very similar overall viscoelastic behavior to MR1. This indicates a more pronounced shear-thinning behavior. In contrast, the addition of EOC in turns increases η^* of the model recycled blends at higher frequencies, which is an interesting result that should be combined with their morphological characteristics.

The plot of G' *vs.* G'', known as Han's plot and first proposed by Han,[15] was employed to estimate the compatibility of the blends. An increase in G' can be attributed to enhanced entanglements in compatibilized blends, as demonstrated by Jafari *et al.* [Jafari *et al.*] As well, the change in microstructure of the blend can be predicted by the variation of G' *vs.* G'' of the polymers.[14] Fig. 4(e) and (f) show the Han's plot for the model recycled blends compatibilized by EPR and EOC, respectively. As observed, the slopes of the curves for all blends are very similar at lower frequencies. However, at higher frequencies, the compatibilized blend with EPR exhibits a distinct behavior

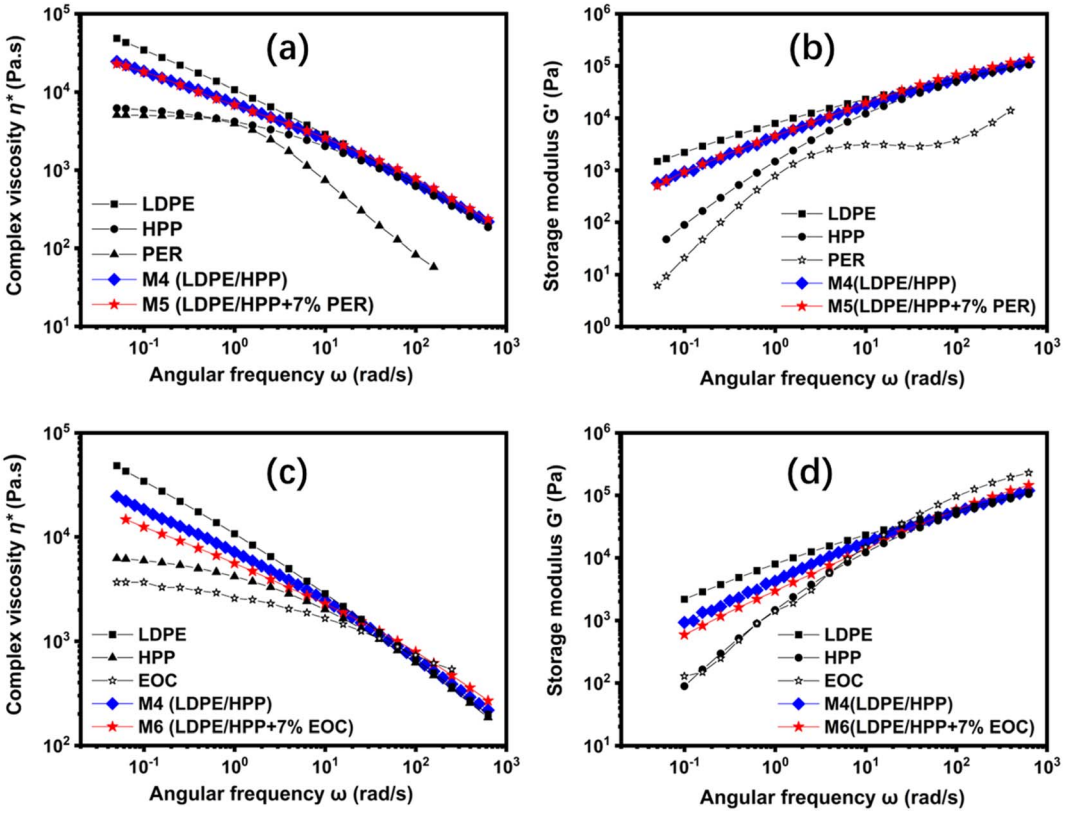

Fig. 3 Plots of complex viscosity (η^*) and storage modules (G') as functions of angular frequency at 200 °C for neat polymers, the LDPE/HPP blend, and their compatibilized blends with EPR (a and b) and EOC (c and d).

compared to the uncompatibilized MR1 blend, indicating a modified morphological structure. At a given G'', MR2 shows the highest G' values indicating increased elasticity, which is attributed to its co-continuous phase structure.[16] Fig. 4(f) illustrates Han's plot for the model recycled blends compatibilized with the EOC. Along the entire frequency range, the slopes remain essentially unchanged after compatibilization, implying that the blend MR3 is less sensitive to frequency changes in presence of EOC. This suggests a more stable morphology and a qualitatively uniform microstructure.

To summarize, for both LLDPE/CPP and LDPE/HPP blends, EOC seems to be the most effective compatibilizer in terms of influencing their rheological properties. Compatibilization is expected to be achieved through the physical affinity of EOC copolymer blocks with each phase, which enhances interfacial adhesion between the components.[17] This hypothesis will be further validated by examining the morphological and mechanical properties of the model blends.

4.2 Morphological observations

The morphology of the model blends was initially examined using SEM and TEM. To enhance the phase contrast, the samples were cryo-ultramicrotomed and chemically stained with ruthenium tetroxide (Ru04) vapor for 2 hours. The LLDPE/CPP blend was selected as a representative system to evaluate the effect of compatibilizers. As shown in Fig. 5(a), the LLDPE and CPP phases are clearly distinguishable and identified. The LLDPE/CPP blend displays a typical sea-island morphology, in which the continuous phase in black corresponds to LLDPE, while the dispersed phase in gray displaying droplet morphology represents CPP domains. When compatibilizer EPR and EOC are introduced, as shown in Fig. 5(b) and (c), respectively, the blends retain a droplet-like structure but with significantly finer morphologies. The incorporation of EPR and EOC results in a substantial reduction in droplet size. Based on the droplet size distribution histogram, the average droplet diameter decreases from approximately 0.1 μm in the uncompatibilized blend (M1) to around to 0.01 μm in the compatibilized systems, indicating a finer morphological structure. This suggests that the compatibilizers used effectively reduce interfacial tension and improve interactions between LLDPE and CPP phases, which is consistent with the rheological results.[17]

Although the M2 and M3 blends present similar average CPP droplet sizes, their different morphological shapes differ notably. Further TEM observations of the compatibilized blends were further performed to analyze these differences in detail. As displayed in Fig. 5(b') and (c'), the CPP domains in M3 blends compatibilized by EOC clearly display a more elongated shape compared to those in the M2 blend compatibilized with EPR. To quantitatively assess this observation, the circularity of the CPP droplets was calculated using the following equation:

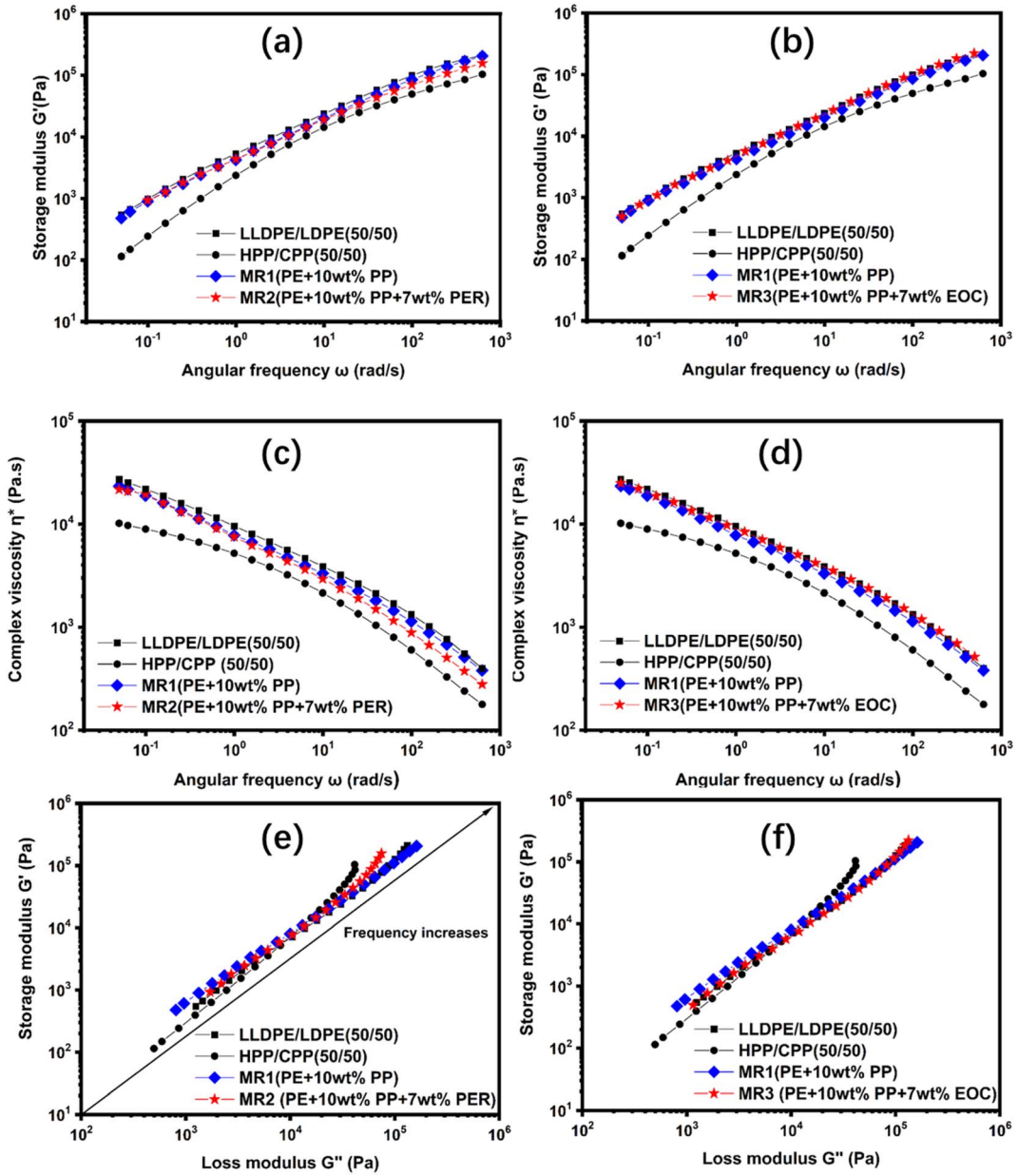

Fig. 4 Plots of complex viscosity (η^*) and storage modules (G') as functions of angular frequency, and Han's plot at 200 °C for binary blends, the model recycled blend, and their compatibilized recycled blends with EPR (a, c and e) and EOC (b, d and f).

$$\text{Circ} = \frac{4 \times \pi \times \text{area}}{\text{perimeter}^2}$$

Here, the data used in the circularity equation were obtained from TEM micrographs. A circularity value of 1.0 indicates a perfect circle, while values approaching to 0.0 present increasingly elongated shapes. Average circularity values of 0.3 and 0.1 were obtained for the M2 and M3 blends, respectively, supporting our observations. Furthermore, the more elongated shape of CPP droplets in the EOC-compatibilized M3 blend provides additional evidence consistent with the rheological results.

Fig. 6(a) and (b) further presents high-vacuum SEM micrographs at different magnifications of the fractured surface of the uncompatibilized quaternary model recycled blends. As observed, MR1 exhibits a complex morphology, composed of a fibrous-structured matrix in black and grey, that were superposed to each other, along with dispersed phases and inclusions in light grey and white with different sizes. This model recycled blend indicates a multi-dispersed droplet structure, in which different phases (both continuous and dispersed) are superimposed to each other.

Low-vacuum SEM and TEM images of the compatibilized model recycled blends MR2 (PE/PP/EPR) and MR3 (PE/PP/EOC) are displayed in Fig. 6(c, d) and (c', d'), respectively. Obviously,

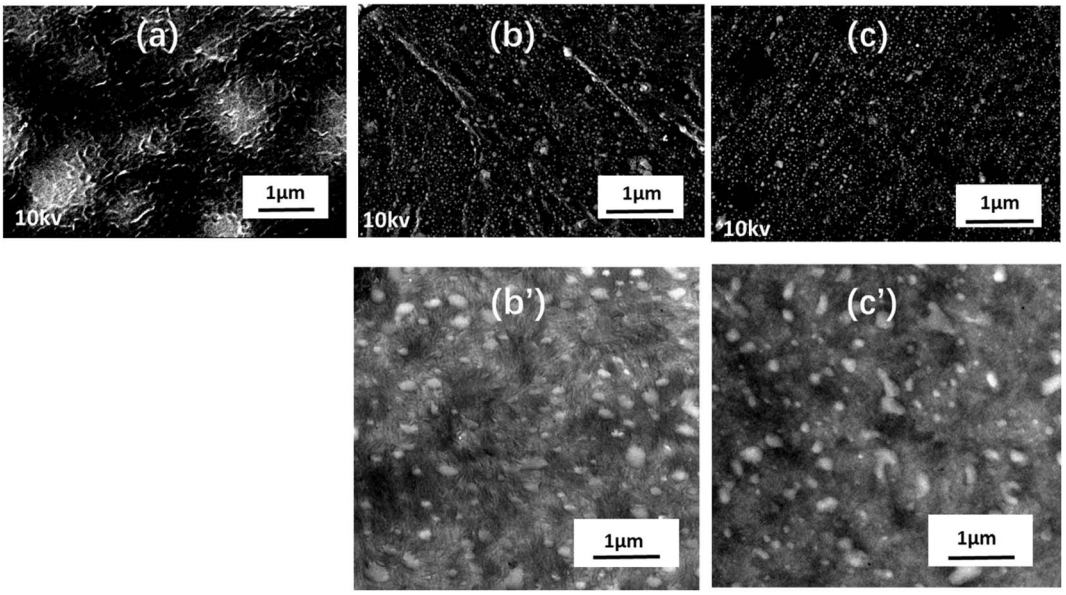

Fig. 5 High-vacuum SEM micrographs for (a) M1 (LLDPE/CPP blend without compatibilizer), (b) M2 (LLDPE/CPP blend with 7 wt% EPR) and (c) M3 (LLDPE/CPP blend with 7 wt% EOC), TEM images of LLDPE/CPP blends with compatibilizers: (b') M2 (LLDPE/CPP/EPR) and (c') M3 (LLDPE/CPP/EOC).

both blends clearly display a finer morphology with significantly reduced dispersed droplet sizes. The presence of the compatibilizer EPR and EOC, results in a more homogeneous distribution of the dispersed phase, with mean droplet sizes of approximately 0.02 μm and 0.05 μm, respectively, which are far below 0.3 μm observed in uncompatibilized MR1 blend. Notably, a distinct 'core–shell' structure is obviously observed, in which the darker regions surrounding the droplets appear to correspond to compatibilizer rich domains. From a thermodynamic point of view, such "onion" type morphologies or multi-dispersed droplet structures is theoretically present to reduce interfacial tension and interactions between immiscible phases. Moreover, PP droplets in the MR3 blend also display a more elongated shape compared to those in MR2. This is quantitatively supported by average circularity value of 0.3 and 0.6 for MR3 and MR2, respectively. These findings are consistent with our previous observations in the model blends. The non-steady state 'fibrous-like' morphology of the dispersed phase in MR3 contributes to an additional elastic response due to shape relaxation, which can greatly explain the observed increase in both complex viscosity (η^*) and storage modulus (G') compared to the uncompatibilized blend. Furthermore, the formation of elongated domains under identical processing conditions suggests lower interfacial tension in complex systems, indicating a relatively better level of compatibilization, compared to the more spherical droplet shape observed in MR2.

In summary, from a morphological perspective, the introduction of both compatibilizers significantly enhances the compatibility between polyethylene (PE) and polypropylene (PP), as evidenced by the notable reduction in droplet size. This reduction suggests decreased interfacial tension and weaker interfacial interactions in systems. Compared to EPR-based blends, EOC-compatibilized blends display a more elongated dispersed phase presenting the improved compatibilization. This can be attributed to the fact that the elongated shape provides a larger interfacial/interphasic area and finer morphology, which correspond to lower interfacial tension at a comparable phase size. Although such elongated structure may not represent a thermodynamic steady state, they reflect a kinetically favorable morphology under the given processing conditions.

4.3 Mechanical properties of model and recycled blends

The impact failure weight histogram of the LLDPE/CPP and LDPE/HPP films, normalized by film thickness, are presented in Fig. 7 and the main data are listed in Table 5. As observed, the incorporation of only 10 wt% PPs significantly reduces the impact failure of both PE types due to their immiscibility. Specifically, the impact failure weight of the LLDPE/CPP blend decreases by 82%, reaching 3.8 ± 1 g μm^{-1}, while that of the LDPE/HPP blend decreases to 2.6 ± 1 g μm^{-1}. The presence of compatibilizer PER has a modest positive effect, improving the impact resistance by approximately 10% in both M1 (4.2 ± 2 g μm^{-1}) and M4 (2.8 ± 1 g μm^{-1}) blends. In contrast, EOC can enhance the impact properties of the model blends by 24% in M1 (4.7 ± 1 g μm^{-1}) and by 42% in M4 (3.7 ± 1 g μm^{-1}), respectively.

The impact failure weight values of the model recycled films, normalized by the film thickness, are further investigated as presented in Table 5. As expected, the combination of LLDPE and LDPE significantly reduces the impact failure weight compared to that of the individual LLDPE and LDPE films. The presence of 10 wt% PP blend (5 wt% HPP+5 wt% CPP) further decreases the impact failure weight of the LLDPE/LDPE blend by 40%, from 7.3 ± 2 g μm^{-1} to 4.1 ± 1 g μm^{-1}. Upon

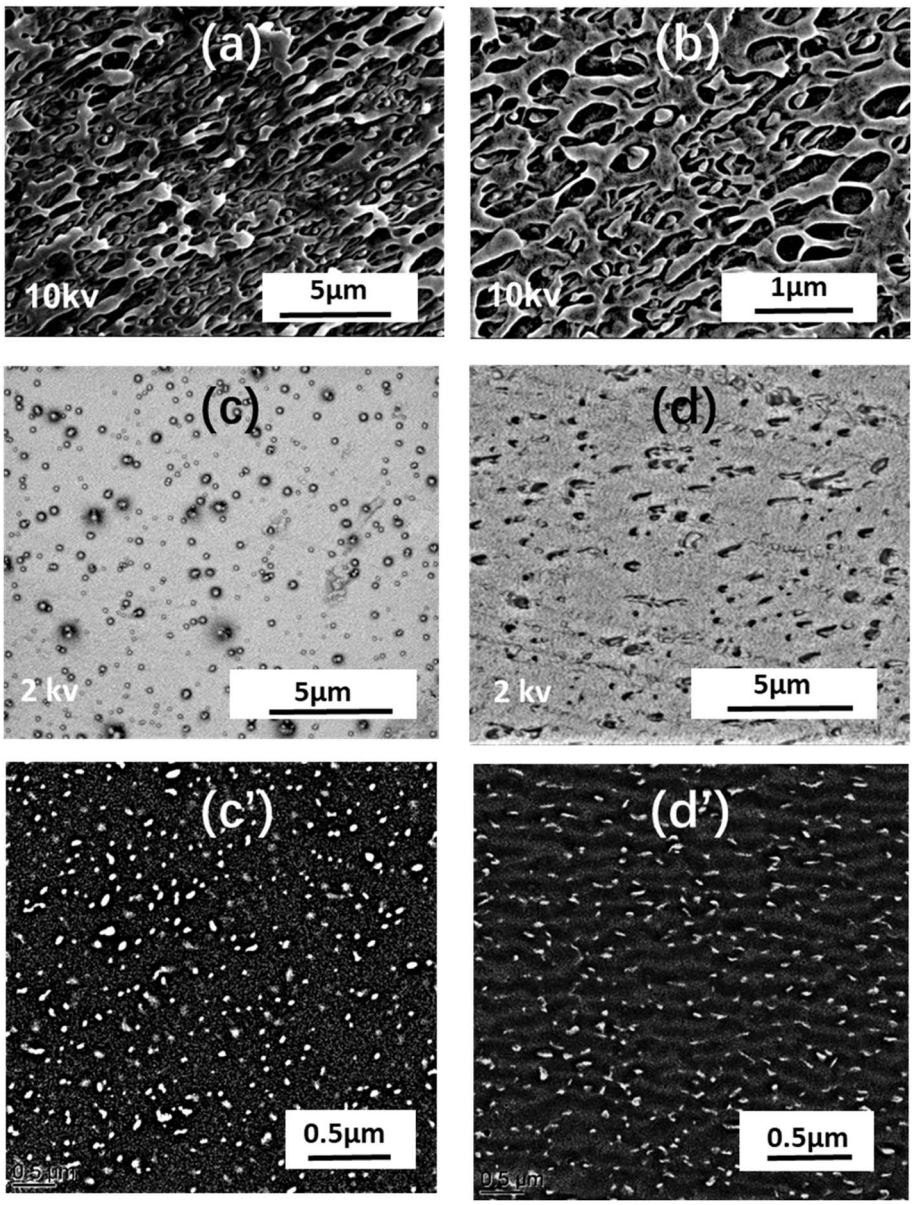

Fig. 6 (a) and (b) High-vacuum SEM images showing the cross-fracture of MR1 model recycled blend at different magnifications. Low-vacuum SEM images of model recycled blends with compatibilizers: (c) MR2 (PE/PP/EPR) and (d) MR3 (PE/PP/EOC). TEM images of LLDPE/CPP blends with compatibilizers: (c') M2 (LLDPE/CPP/EPR) and (d') M3 (LLDPE/CPP/EOC).

compatibilization with either EPR or EOC, the impact properties of the blends remarkably improve, reaching 6.6 ± 1 g μm^{-1} and 9.1 ± 1 g μm^{-1}, respectively, which are comparable to those observed in the model blends. These results suggest that EOC due to its molecular structure of ethylene–octene segments, greatly enhances not only the interfacial adhesion between the PE and PP phases but also the overall impact resistance of the recycled blends.

Since cracks are more likely to initiate and propagate in machine direction (MD), the mechanical failure of the films is closely related to film orientation.[18] Therefore tear resistance was evaluated in both machine direction (MD) and transverse direction (TD). The tear resistance values of the LLDPE/CPP and LDPE/HPP blends, normalized by the film thickness, are summarized in Table 6. As shown, neat LDPE presents slightly higher tear resistance in the MD (9.4 ± 1 cN μm^{-1}) compared to neat LLDPE (6.7 ± 1 cN μm^{-1}). However, in TD, LLDPE displays significantly higher value (27.7 ± 4 cN μm^{-1}) than LDPE (12.6 ± 2 cN μm^{-1}). This is attributed to the higher degree of short-chain branching and lower long-chain branching in LLDPE, which is expected to enhance tear strength relative to LDPE.[19] Then, the presence of CPP and HPP into LLDPE and LDPE blends, respectively, results in a significant reduction in tear resistance. Specifically, for the LLDPE/CPP blend, tear resistance drops to 3.1 ± 1 cN μm^{-1} in the TD and 3.3 ± 1 cN μm^{-1} in the MD, which are approximately 90% and 50% loss in the tear

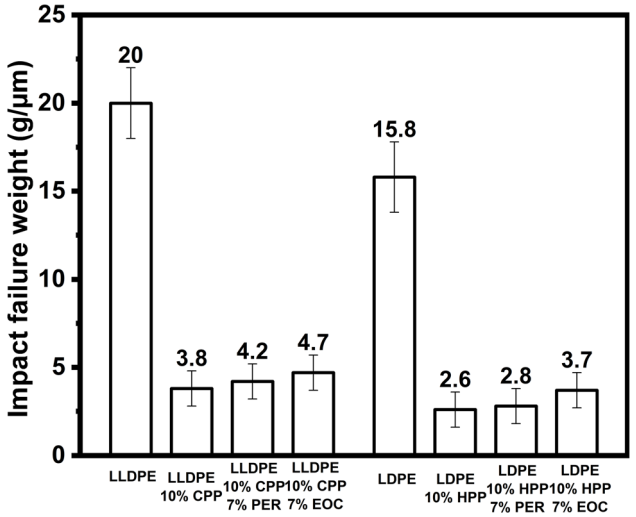

Fig. 7 Histogram of impact failure weight for neat polymers, model blends, and compatibilized blends.

Table 5 The impact failure weight of the neat polymers and model blends with effect of compatibilizers

Samples	Impact failure weight (g μm^{-1})
100%LLDPE	20.6 ± 2
M1: 90%LLDPE + 10%CPP	3.8 ± 1
M2: 83%LLDPE + 10%CPP + 7%EPR	4.2 ± 1
M3: 83%LLDPE + 10%CPP + 7%EOC	4.7 ± 1
100%LDPE	15.8 ± 2
M4: 90%LDPE + 10%HPP	2.6 ± 1
M5: 83%LDPE + 10%HPP + 7%EPR	2.8 ± 1
M6: 83%LDPE + 10%HPP + 7%EOC	3.7 ± 1
50%LLDPE1 + 50%LDPE	7.3 ± 2
MR1: 90%PEs + 10%PPs	4.1 ± 1
MR2: 83%PEs + 10%PPs + 7%EPR	6.6 ± 1
MR3: 83%PEs + 10%PPs + 7%EOC	9.1 ± 1

Table 6 Tear resistance of LLDPE, LDPE and their blends in the machine direction (MD) and transverse direction (TD)

Films	MD (cN μm^{-1})	TD (cN μm^{-1})
100%LLDPE	6.7 ± 1	27.7 ± 2
M1: 83%LLDPE + 10%CPP	3.3 ± 1	3.1 ± 1
M2: 83%LLDPE + 10%CPP + 7%EPR	4.7 ± 0.5	8.9 ± 0.5
M3: 83%LLDPE + 10%CPP + 7%EOC	5.5 ± 0.5	9.9 ± 0.5
100%LDPE	9.4 ± 1	12.6 ± 2
M4: 90%LDPE + 10%HPP	0.8 ± 0.1	1.5 ± 0.1
M5: 83%LDPE + 10%HPP + 7%EPR	1.6 ± 0.1	5.5 ± 0.5
M6: 83%LDPE + 10%HPP + 7%EOC	2.0 ± 0.1	7.5 ± 0.5
50%LLDPE + 50%LDPE	3.2 ± 0.5	17.4 ± 2
MR1: 90%PEs + 10%PPs	1.4 ± 0.1	1.0 ± 0.1
MR2: 83%PEs + 10%PPs + 7%EPR	1.5 ± 0.1	14.4 ± 0.5
MR3: 83%PEs + 10%PPs + 7%EOC	2.2 ± 0.1	16.5 ± 0.5

strength, respectively, compared to neat LLDPE. In the case of the LDPE/HPP blend, the presence of HPP leads to a dramatic decrease in tear resistance in MD by 92% (0.8 ± 0.1 cN μm^{-1}), and by 88% in the TD (1.5 ± 0.1 cN μm^{-1}). Overall, the presence of HPP and CPP significantly decreases the tear performances of the polyethylene films mostly in both orientations.

Furthermore, the effect of EPR and EOC compatibilizers on the tear resistance of the blends in both the MD and TD directions is also presented in Table 6. For the LLDPE/CPP blends, the addition of EPR and EOC increases tear resistance by 42% and 67% in the MD direction, and by 187% and 219% in TD direction, respectively. In the case of the LDPE/HPP blends, EPR and EOC significantly improve tear resistance by 100% and 150% in the MD, and by 266% and 400% in TD direction, respectively. These results clearly indicate that EOC is a more effective compatibilizer than EPR in enhancing tear resistance.

The tear resistance values of the model recycled films, normalized by the film thickness, are displayed in Table 6. As observed, the overall trend for the model recycled films is consistent with that of the previously discussed model blends. Firstly, the LLDPE/LDPE (50/50) exhibits a significantly lower tear resistance in the MD direction (3.2 ± 0.5 cN μm^{-1}) compared to the neat LLDPE and LDPE films. This reduction is attributed to poor compatibility between the two types of polyethylene, which was also observed in the dart impact test results. Then, the presence of 10 wt% PP (5 wt% HPP+5 wt% CPP) into the blends further reduces tear resistance in the MD by 56% relative to the LLDPE/LDPE (50/50) blend, and results in a dramatic 94% decrease in the TD direction. In contrast, the addition of the compatibilizers significantly improves tear performance. In the TD direction, EPR and EOC increase the tear resistance of the MR1 blend (1.0 ± 0.1 cN μm^{-1}) by 1200% and 1400%, respectively, yielding 14.4 ± 0.5 cN μm^{-1} for MR2 and 16.5 ± 0.5 cN μm^{-1} for MR3. In the MD direction, EPR has little effect, while EOC enhances tear strength in MD direction by 57%, increasing it to 2.2 ± 0.1 cN μm^{-1}. These results clearly demonstrate that ethylene–octene copolymer (EOC) is the most effective among those studied, significantly enhancing the interfacial adhesion between the PE and PP phases and thereby improving both impact and tear strength in the model recycled blends.

Tensile tests of the model recycled films were finally performed in the machine direction (MD). The main critical data including the tensile strength, tensile strength at break and elongation at break were summarized in Table 7. The inclusion of PP into the PE blend results in an increase in tensile stress at yield but a noticeable decrease in both elongation at break and tensile stress at break, indicating a more brittle behavior. Specifically, the MR1 film exhibits an elongation at break of 228.1 ± 35%, representing a 59% reduction compared to 562.6 ± 30% for the LLDPE/LDPE blend. This finding is consistent with the observed reduction in impact strength, as previously discussed, and can be attributed to the incompatibility between PP and PE, as well as the inherently lower toughness of PP. For the compatibilized blends, the addition of the EPR and EOC can enhance the elongation at break of model recycled blends while slightly reducing the tensile strength at break, as expected. Overall, EOC proves to be the most effective compatibilizer, improving not only the impact and tear strength but also deformability, due to its elastic feature and strong compatibilization effect between the PP and PE phases.

Table 7 Mechanical properties of uncompatibilized and compatibilized model recycled films, including tensile strength at yield, tensile strength at break and elongation at break

Samples	Tensile strength at yield (MPa)	Tensile strength at break (MPa)	Elongation at break (%)
50% LLDPE + 50% LDPE	6.7 ± 0.6	44.3 ± 6	562.6 ± 30
MR1: 90%PEs + 10%PPs	8.2 ± 0.5	19.5 ± 2	228.1 ± 35
MR2: 83%PEs + 10%PPs + 7%EPR	3.6 ± 0.4	17.9 ± 3	228.5 ± 29
MR3: 83%PEs + 10%PPs + 7%EOC	2.19 ± 0.2	16.4 ± 4	240.0 ± 48

Conclusion

In the context that polyethylene (PE)-based agricultural waste films are often contaminated with small amounts of polypropylene (PP) during the recycling process, the recycled mixtures result in poor mechanical performance due to the immiscibility between the multi-components in such multiphase systems. To the best of our knowledge, few studies have systematically investigated multiphase blend systems based on designed PE/PP compositions. In this study, physical compatibilization was employed to enhance the mechanical performance of such complex mechanically recycled systems. The compatibilization effects of propylene–ethylene elastomer (EPR) and ethylene–octene copolymer (EOC) were examined in model binary PE/PP blends, as well as quaternary model recycled PE/PP blends incorporating virgin LLDPE, LDPE, and PP. The rheological, morphological and mechanical properties, along with their interrelationships, were comprehensively analyzed. Both compatibilizers significantly enhanced the compatibility between PE and PP, as evidenced by reductions in complex viscosity and elastic modulus, particularly at lower frequencies. Scanning electron microscopy (SEM) and transmission electron microscopy (TEM) revealed significantly finer morphologies and reduced dispersed domain sizes in the compatibilized systems, which further support the rheological findings. Specifically, the presence of the compatibilizer EPR and EOC, contributed to mean droplet sizes of approximately 0.02 μm and 0.05 μm, respectively, which are far below 0.3 μm observed in uncompatibilized blend. As a result of improved interfacial adhesion, notable enhancements in impact resistance, tear resistance, and elongation at break were observed. In summary, both compatibilizers effectively diminished interfacial/interphase interaction in the studied multiphase recycled systems. Moreover, EOC was found to be the most efficient compatibilizer compared to EPR, particularly in the model recycled blends with such PE/PP compositions. A morphology-rheology-property relationship was systematically established to elucidate the physical compatibilization mechanism in complex multiphase systems. These findings provide practical guidance for improving mechanical performance of recycled PE-based agricultural waste films through compatibilization strategies.

Author contributions

All authors have read and approved the final version of the manuscript. H. Q: Conceptualization, data curation, software, formal analysis, investigation, visualization, writing – review & editing. G. C: Data curation, formal analysis, investigation, visualization, methodology, writing – original draft. A. M: Resources, supervision, funding acquisition, validation, administration, writing – review & editing. K. L: Resources, supervision, funding acquisition, validation, administration, writing – review & editing.

Conflicts of interest

No potential conflict of interest was reported by the author(s).

Data availability

The analysis codes and data can be provided on request.

Acknowledgements

The authors thank financial support from the Région Auvergne-Rhône-Alpes Council (ARC, AURA 2017–2020), the MESRI (Ministère de l'Enseignement Supérieur, de la Recherche et de l'Innovation), and PIA France 2030 and the French National Research Agency (ANR) through the PEPR program Plastics 22-PERE-0002.

References

1 Z. O. Schyns and M. P. Shaver, Mechanical recycling of packaging plastics: a review, *Macromol. Rapid Commun.*, 2021, **42**(3), 2000415.
2 K. B. Biji, C. N. Ravishankar, C. O. Mohan and T. K. Srinivasa Gopal, Smart packaging systems for food applications: a review, *J. Food Sci. Technol.*, 2015, **52**, 6125–6135.
3 K. Ragaert, L. Delva and K. Van Geem, Mechanical and chemical recycling of solid plastic waste, *Waste Manage.*, 2017, **69**, 24–58.
4 I. Kyrikou and D. Briassoulis, Biodegradation of agricultural plastic films: a critical review, *J. Polym. Environ.*, 2007, **15**, 125–150.
5 D. Briassoulis, M. Hiskakis, G. Scarascia, P. Picuno, C. Delgado and C. Dejean, Labeling scheme for agricultural plastic wastes in Europe, *Qual. Assur. Saf. Crops Foods.*, 2010, **2**(2), 93–104.
6 J. Maris, S. Bourdon, J. M. Brossard, L. Cauret, L. Fontaine and V. Montembault, Mechanical recycling: Compatibilization of mixed thermoplastic wastes, *Polym. Degrad. Stabil*, 2018, **147**, 245–266.

7 G. Suzuki, N. Uchida, K. Tanaka, H. Matsukami, T. Kunisue, S. Takahashi and M. Osako, Mechanical recycling of plastic waste as a point source of microplastic pollution, *Environ. Pollut.*, 2022, **303**, 119114.
8 X. Zhang, Y. Xu, X. Zhang, H. Wu, J. Shen, R. Chen and S. Guo, Progress on the layer-by-layer assembly of multilayered polymer composites: Strategy, structural control and applications, *Prog. Polym. Sci.*, 2019, **89**, 76–107.
9 G. Cabrera, J. Li, A. Maazouz and K. Lamnawar, A Journey from Processing to Recycling of Multilayer Waste Films: A Review of Main Challenges and Prospects, *Polymers*, 2022, **14**, 2319.
10 S. Bertin and J. J. Robin, Study and characterization of virgin and recycled LDPE/PP blends, *Eur. Polym. J.*, 2002, **38**(11), 2255–2264.
11 C. Fang, L. Nie, S. Liu, R. Yu, N. An and S. Li, Characterization of polypropylene–polyethylene blends made of waste materials with compatibilizer and nano-filler, *Compos Part B-eng.*, 2013, **55**, 498–505.
12 J. W. Teh, A. Rudin, S. Y. Yuen, J. C. Keung and D. M. Pauk, LLDPE/PP blends in tubular film extrusion: Recycling of mixed films, *J. Plast. Film Sheeting*, 1994, **10**(4), 288–301.
13 S. Vervoort, J. Den Doelder, E. Tocha, J. Genoyer, K. L. Walton, Y. Hu and K. Jeltsch, Compatibilization of polypropylene–polyethylene blends, *Polym. Eng. Sci.*, 2018, **58**(4), 460–465.
14 R. Krache, D. Benachour and P. Pötschke, Binary and ternary blends of polyethylene, polypropylene, and polyamide 6, 6: The effect of compatibilization on the morphology and rheology, *J. Appl. Polym. Sci.*, 2004, **94**(5), 1976–1985.
15 H. K. Chuang and C. D. Han, Rheological behavior of polymer blends, *J. Appl. Polym. Sci.*, 1984, **29**(6), 2205–2229.
16 S. H. Jafari, P. Pötschke, M. Stephan, H. Warth and H. Alberts, Multicomponent blends based on polyamide 6 and styrenic polymers: morphology and melt rheology, *Polymer*, 2002, **43**(25), 6985–6992.
17 Y. Kazemi, A. Ramezani Kakroodi and D. Rodrigue, Compatibilization efficiency in post-consumer recycled polyethylene/polypropylene blends: Effect of contamination, *Polym. Eng. Sci.*, 2015, **55**(10), 2368–2376.
18 Y. Ren, Y. Shi, X. Yao, Y. Tang and L. Z. Liu, Different dependence of tear strength on film orientation of LLDPE made with different co-monomer, *Polymers*, 2019, **11**(3), 434.
19 A. Peacock, *Handbook of Polyethylene: Structures: Properties, and Applications*, CRC press, 2002.